ARTICLES
https://doi.org/10.1038/s41588-021-00968-y

nature genetics

Mendelian randomization analyses support causal relationships between blood metabolites and the gut microbiome

Xiaomin Liu[1,2,8], Xin Tong[1,8], Yuanqiang Zou[1], Xiaoqian Lin[1,2], Hui Zhao[1,2], Liu Tian[1], Zhuye Jie[1], Qi Wang[1,2], Zhe Zhang[1], Haorong Lu[3], Liang Xiao[1,4,5], Xuemei Qiu[1], Jin Zi[1], Rong Wang[1], Xun Xu[1], Huanming Yang[1,6], Jian Wang[1,6], Yang Zong[1], Weibin Liu[1], Yong Hou[1], Shida Zhu[1], Huijue Jia[1,7] ✉ and Tao Zhang[1] ✉

The gut microbiome has been implicated in a variety of physiological states, but controversy over causality remains unresolved. Here, we performed bidirectional Mendelian randomization analyses on 3,432 Chinese individuals with whole-genome, whole-metagenome, anthropometric and blood metabolic trait data. We identified 58 causal relationships between the gut microbiome and blood metabolites, and replicated 43 of them. Increased relative abundances of fecal *Oscillibacter* and *Alistipes* were causally linked to decreased triglyceride concentration. Conversely, blood metabolites such as glutamic acid appeared to decrease fecal *Oxalobacter*, and members of *Proteobacteria* were influenced by metabolites such as 5-methyltetrahydrofolic acid, alanine, glutamate and selenium. Two-sample Mendelian randomization with data from Biobank Japan partly corroborated results with triglyceride and with uric acid, and also provided causal support for published fecal bacterial markers for cancer and cardiovascular diseases. This study illustrates the value of human genetic information to help prioritize gut microbial features for mechanistic and clinical studies.

Metagenome-wide association studies (MWAS) using human stool samples, as well as animal models, especially germ-free mice, have pointed to a potential role of the gut microbiome in conditions such as cardiometabolic diseases, autoimmune diseases, neuropsychiatric disorders and cancer, with mechanistic investigations for diseases such as obesity, colorectal cancer and schizophrenia[1–4]. Twin-based heritability estimation and more recent metagenome-genome-wide association studies (M-GWAS) have questioned the traditional view of the gut microbiota as a purely environmental factor[5–9], although the extent of the genetic influence remains controversial[7,10]. Yet, all these published cohorts, except for human sequences in the metagenomic data of the Human Microbiome Project (HMP), used array data for human genetics, and most of them had 16 S rRNA gene amplicon sequencing for the fecal microbiota[5–9].

As the gut microbiome is considered to be highly dynamic, causality has been an unresolved issue in the field. Mendelian randomization (MR)[11] offers an opportunity to distinguish between causal and noncausal effects from cross-sectional data, without animal studies or randomized controlled trials. An early study used MR to look at the gut microbiota and ischemic heart disease[12]. Recently, a study used MR to confirm that increased relative abundance of bacteria producing the fecal volatile short-chain fatty acid (SCFA) butyrate was causally linked to improved insulin response to oral glucose challenge; in contrast, another fecal SCFA, propionate, was causally related to an increased risk of type 2 diabetes (T2D)[13]. However, both studies used genotype data, and it was not clear to what extent the genetic factors explained the microbial feature of interest.

In this study, we present a large-scale M-GWAS using whole-genome and fecal microbiome, followed by bidirectional MR (BMR) for the fecal microbiome and anthropometric features as well as blood metabolites. In a two-stage design from different cities in China, we identified 58 causal links from MR in the 4D-SZ (multiomics, with more time points to come, from Shenzhen, China) discovery cohort of 2,002 individuals with high-depth whole-genome sequencing data (1,539 individuals with microbiome data for one-sample MR). We replicated 43 of the 58 causal effects using low-depth whole-genome sequencing data of another 1,430 individuals (1,006 individuals with microbiome data for one-sample MR). In general, unidirectional causal effects could be found both from the gut to the blood and from the blood to the gut, but bidirectional effects were rarely detected. A few of the M-GWAS associations with gut microbial functional modules, for example, module for lactose/galactose degradation and the *ABO* loci, reached study-wide significance, illustrating the power of shotgun metagenomic data together with whole-genome sequencing (WGS). The MR findings were corroborated and extended by summary statistics from the Biobank Japan study; for example, causal effect of *Proteobacteria* on T2D, congestive heart disease and colorectal cancer, underscoring the significance of human genetic data to help guide microbiome intervention studies.

[1]BGI-Shenzhen, Shenzhen, China. [2]College of Life Sciences, University of Chinese Academy of Sciences, Beijing, China. [3]China National Genebank, BGI-Shenzhen, Shenzhen, China. [4]Shenzhen Engineering Laboratory of Detection and Intervention of Human Intestinal Microbiome, BGI-Shenzhen, Shenzhen, China. [5]BGI-Qingdao, BGI-Shenzhen, Qingdao, China. [6]James D. Watson Institute of Genome Sciences, Hangzhou, China. [7]Shenzhen Key Laboratory of Human Commensal Microorganisms and Health Research, BGI-Shenzhen, Shenzhen, China. [8]These authors contributed equally: Xiaomin Liu, Xin Tong. ✉e-mail: jiahuijue@genomics.cn; tao.zhang@genomics.cn

Results

Fecal microbiome features associated with human genetic variants. We set out to identify human genetic variants to be included as the randomizing layer of MR (Fig. 1). The 4D-SZ discovery cohort consisted of high-depth whole-genome sequencing data from 2,002 blood samples (mean depth of 42×; Supplementary Table 1 and Supplementary Fig. 1a), out of which 1,539 individuals had metagenomic shotgun sequencing data from stool samples (8.56 ± 2.28 Gb; Supplementary Fig. 1b). We carried out fecal M-GWAS using 10 million common and low-frequency variants (minor allele frequency (MAF) ≥0.5%) and 500 unique microbial features (Spearman's correlation <0.99; Methods). The M-GWAS was adjusted for age, gender, body mass index (BMI), defecation frequency, stool form, self-reported diet, lifestyle factors and the first four principal components (PCs) from the genomic data to account for population stratification.

With this large cohort of whole-genome and whole-metagenome data, we performed M-GWAS analysis and identified a total of 625 associations involving 548 independent loci for 1 or more of the 500 microbial features at genome-wide significance ($P < 5 \times 10^{-8}$). With a more conservative Bonferroni-corrected study-wide significant P value of 1.0×10^{-10} ($=5 \times 10^{-8}/500$), we identified 28 associations with fecal microbial features involving 27 genomic loci, of which 5 correlated with gut bacteria and the other 22 associated with gut metabolic pathways (Supplementary Table 2).

For MR, it was important for the genetic variants used to be representative of the microbiome features (Supplementary Fig. 2), so a more suggestive P value of less than 1×10^{-5} was used (Supplementary Table 2), as in previous MR studies[13,14]. Each microbial feature had an average of 44 genetic variants (Fig. 2a and Supplementary Table 3). The corresponding genetic variants explained microbial features to a median value of 24.9%, for example, 45.5% of the microbial metabolic pathway for succinate consumption and 44.6% of *Phascolarctobacterium succinatutens* (an asaccharolytic, succinate-utilizing bacterium), while only 6.8% of genus *Edwardsiella* (Supplementary Table 3). The phenotypic (relative abundance) variance of five genera (*Bilophila*, *Oscillibacter*, *Faecalibacterium*, *Megasphaera* and *Bacteroides*) could be explained over 35% by their corresponding independent genetic variants (Fig. 2b). Thus, although human genetic associations (array data) have been reported to explain only 10% or 1.9% of the gut microbiota[7,10], the suggestive associations from the current M-GWAS study could be highly predictive of certain gut taxa and functions.

For better confidence in these suggestive associations, we sequenced a replication cohort of 1,430 individuals from multiple cities in China (also shotgun metagenomic sequencing for stool samples, but about eight times whole-genome sequencing for human genome; Supplementary Fig. 1c,d). Among the 22,293 independent associations identified in the discovery cohort with $P < 10^{-5}$, 4,876 variants were not available in the low-depth replication dataset and 87.6% of them were not common variants (MAF <0.05). We were able to replicate 2,324 of the remaining 17,417 independent associations in the same effect direction of minor allele ($P < 0.05$; Supplementary Table 2), indicating that the associations were not random false positives. The fraction of associations replicated in the same direction ($P < 0.05$) using the suggestive cut-off of $P < 10^{-5}$ (2,324/17,417) was not lower than the more stringent cut-offs (54/625 of the $P < 5 \times 10^{-8}$, and 2/28 of the $P < 10^{-10}$). Two well-replicated signals from the study-wide threshold were rs1461780285 in the *ABO* blood group associated with module MF0007: lactose and galactose degradation ($P_{discovery} = 2.10 \times 10^{-12}$ and $P_{replication} = 1.09 \times 10^{-10}$; Supplementary Fig. 3a,b) and rs142693490 near the *LCORL* gene (implicated in spermatogenesis, body frame and height) associated with MF0034: alanine degradation II ($P_{discovery} = 1.28 \times 10^{-12}$ and $P_{replication} = 0.014$; Supplementary Fig. 3c,d). Genetic variant rs1461780285 is in strong linkage disequilibrium (LD, $r^2 = 0.99$) with multiple single nucleotide polymorphisms (SNPs) (rs507666, rs532436, rs651007, rs579459 and rs579459) in the *ABO* gene. These SNPs located in a block were found to be associated with metabolites levels in both this and previous studies, especially for serum alkaline phosphatase levels (Supplementary Table 4). In addition, we were able to replicate several previously reported microbial signals[6–10], especially for rs12354611 and *Bacteroides stercoris* ($P = 8.64 \times 10^{-6}$; Supplementary Table 5 and Supplementary Note).

Blood metabolic traits associated with human genetic variants. On the other hand, plasma metabolite levels are also known to associate with host genetic variants (Fig. 1). We thus performed whole-genome-wide association tests for each of the 112 metabolites, with log-transformed relative concentration. We identified a total of 174 associations involving 158 loci that associated independently with 1 or more of the 112 metabolites at genome-wide significance ($P < 5 \times 10^{-8}$). With a more conservative Bonferroni-corrected study-wide significant P value of 4.5×10^{-10} ($= 5 \times 10^{-8}/112$ metabolites), we identified 39 associations with metabolites involving 28 genomic loci (Supplementary Table 6). These included previously well-established associations such as the *UGT1A* family associated with serum total bilirubin[15,16] and *ASPG* associated with asparaginate[15].

According to the suggestive threshold of $P < 10^{-5}$, we identified 6,541 metabolic quantitative trait loci, of which 361 were associated with two or more metabolites (Supplementary Table 6). The average number of genetic variants for each metabolic trait was 58 (Fig. 3a and Supplementary Table 7). The percentage of variance explained by the corresponding genetic variants ranged from 13.3% (red blood cell distribution) to as high as 48.3% (blood mercury concentration) and 45.9% (blood alpha-fetoprotein value), with a median value of 28.6% (Fig. 3b). Among these, 268 variants or their proxy variants ($r^2 > 0.6$; distance <1 Mb) have been reported in the GWAS catalog[17] (Supplementary Table 8). Some variants were associated with diseases in the GWAS catalog such as chronic kidney disease, Alzheimer's disease, coronary artery disease, Crohn's disease, ovarian cancer, breast cancer and gastric cancer.

Among the 6,541 suggestive metabolic quantitative trait loci identified in the 4D-SZ discovery cohort with $P < 10^{-5}$, 5,088 variants were covered by the replication dataset; 717 and 31 were replicated at nominal ($P < 0.05$) and suggestive ($P < 10^{-5}$) significance, respectively, in the same effect direction of minor allele (Supplementary Table 6). Especially for the 174 genome-wide and 39 study-wide significant associations, we could replicate 51 and 29 associations in the same direction ($P < 0.05$), respectively. The top associations confirmed by the low-depth genomes ($P < 4.5 \times 10^{-10}$ both in discovery and replication cohorts) included: *FECH* associated with manganese; *UGT1A* family associated with serum total bilirubin as well as direct and indirect (unconjugated) bilirubin; *ASPG* associated with asparagine; *CPS1* associated with glycine; and *APOE* associated with low density lipoprotein (Supplementary Fig. 4). Overall, the accurate identification of genetic determinants and the high variance explained for both microbial features and blood metabolites are optimal for MR analysis to investigate causality.

From observational correlation to MR. As a prerequisite for strong causality, we investigated the correlation between relative abundances of 500 unique fecal microbial features (taxa and functional modules) and 112 host metabolic traits using multivariate linear regression. After adjustment for gender and age, we observed 457 significant associations (false discovery rate (FDR) corrected $P < 0.05$; Supplementary Table 9 and Methods). Three metabolites, glutamic acid, 5-methyltetrahydrofolic acid (5-methyl THF, active form of folic acid) and selenium, were associated with the largest number of microbial features (58, 40 and 38, respectively; Supplementary Fig. 5). These associations extend findings from

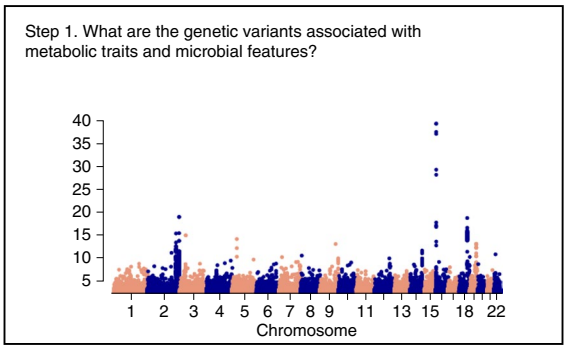

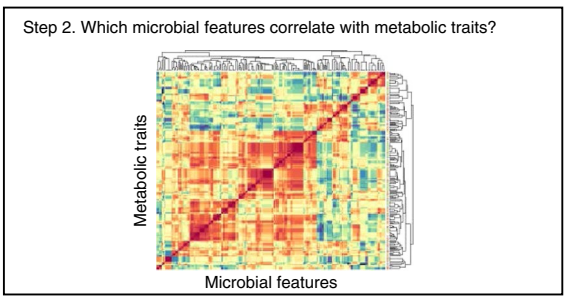

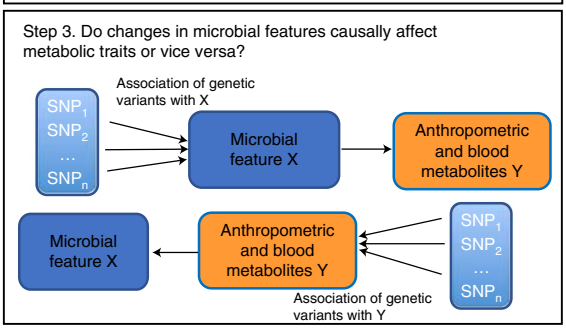

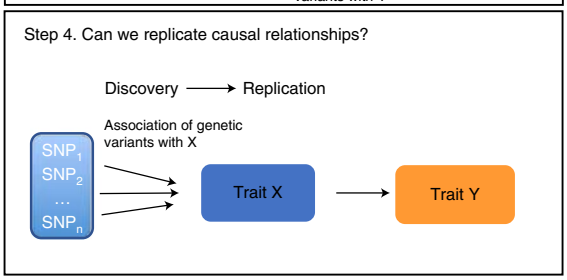

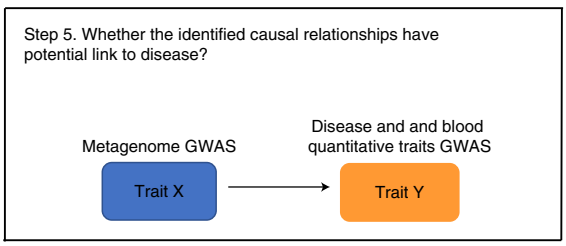

Discovery cohort: 2,002 samples with anthropometric and blood metabolites and high-depth whole genome, 1,539 of which with gut metagenome; 10 million common and low-frequency variants (MAF >0.005; HWE $P > 10^{-5}$; variants calling rate >0.98)

Replication cohort: 1,430 samples with anthropometric and blood metabolites and low-depth whole genome, 1,006 of which with gut metagenome; 5.9 million common and low-frequency variants (MAF >0.005; HWE $P > 10^{-5}$; variants calling rate >0.98)

Metagenome and metabolome GWAS detected genetic variants associated with microbial features and metabolic traits, respectively.

A total of 3,432 samples with anthropometric and blood metabolic traits and whole-genome data, of which 2,545 samples with gut metagenome

Identifying 457 observationally significant associations between 500 unique microbial features and 112 anthropometric and blood metabolites at a FDR-adjusted $P < 0.05$ using a multivariable linear regression analysis

One-sample BMR detected 58 causal associations between microbial features and blood metabolites after multiple test correction ($P < 1.09 \times 10^{-4}$); two-sample BMR detected the same associations and an additional 14 associations

17 causal associations from gut microbiome to blood metabolites involving 12 microbial features and 8 blood metabolites two taxa, genus *Oscillibacter* and *Alistipes* decreased triglyceride amounts

41 causal associations from blood metabolites to gut microbiome involving 7 blood metabolites and 33 microbial features

43 of the 58 causal associations were replicated in the same directions and $P < 0.05$ in an independent sample of replication cohort, for example, genus *Oscillibacter* and *Alistipes* consistently decreased triglyceride amounts

Two-sample MR using metagenome GWAS summary data in this study, together with disease and blood quantitative traits GWAS summary data from Biobank Japan study

We replicate the causal effect of uric acid on increased species unclassified *Lachnospiraceae* bacterium 9_1_43BFAA abundance

Some gut bacteria potentially linked to disease risk

Fig. 1 | Study design and workflow. This schematic representation highlights, for each step, the research question that we sought to answer, the analysis workflow, the data used and the generalized result. We first performed metagenome and metabolome GWAS to detect genetic variants associated with microbial features and metabolic traits, respectively, both in discovery and replication cohorts (Step 1). We then performed observational analysis to identify which microbial feature (taxa, GMM) correlated with metabolic traits in this cohort (Step 2). We used 2,545 samples with information of both microbial features and metabolic traits. We observed 457 significant associations between 500 unique microbial features and 112 anthropometric and blood metabolic traits at an FDR-adjusted $P < 0.05$. We then estimated causal relationships for the 457 observational associations through BMR analysis in the discovery cohort (Step 3). One-sample BMR detected 58 causal associations between microbial features and blood metabolites after multiple test correction ($P < 1.09 \times 10^{-4}$); two-sample BMR detected the same associations and another 14 associations. As a validation, we replicated the discovered causal relationships by using the same MR analysis in an independent replication cohort (Step 4). Over half (43) of the 58 causal associations were replicated in the same direction ($P < 0.05$). Finally, we used two-sample MR analysis to investigate the effects of the identified 72 causal relationships on diseases from the Biobank Japan study (Step 5).

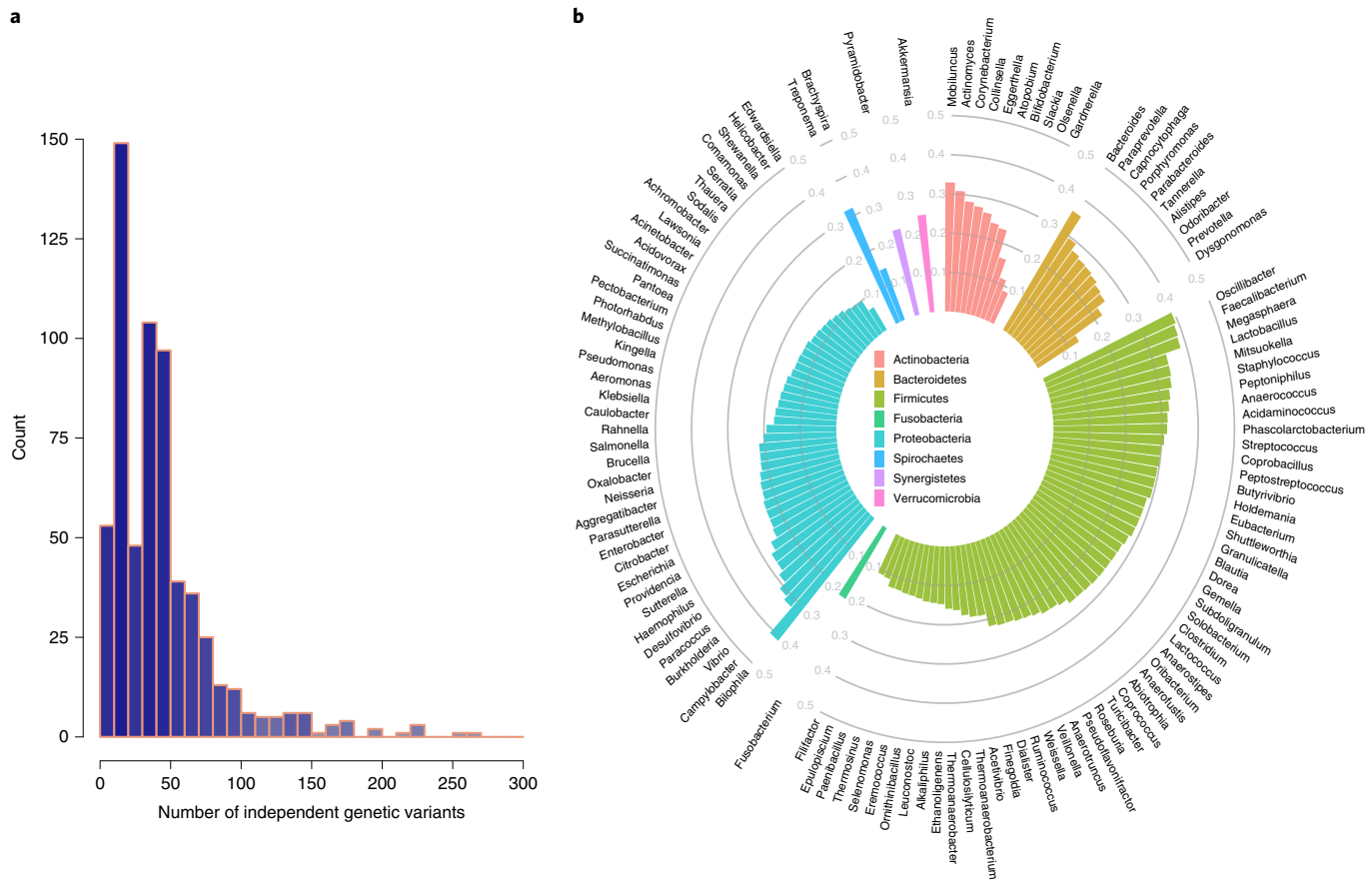

Fig. 2 | Independent genetic variants and their explained variance of microbial features. a, Density plot showing the distribution of number of independent genetic variants that associated with each microbial feature ($r^2 < 0.1$ and $P < 1 \times 10^{-5}$), as calculated by GWAS analysis for a total of 500 unique microbial features. The *x* axis indicates the number of independent genetic variants for each microbial feature (taxon or GMM). The *y* axis indicates the number of microbial features under a given number of independent predictors. **b**, Variance explained by the corresponding independent genetic variants for each microbial feature. The polar bar plot indicates how much the independent genetic variants of each common genus (appeared in at least 50% of samples) explained for their phenotypic variance (relative abundance of each genus). Genera were classified according to their respective phyla, which are marked with different colors. The h^2 was calculated using the REML method in GCTA tools[42].

various studies, and suggest quantitative relationships between gut microbial taxa/functions and plasma metabolites.

As we were fortunate to have all the data in the same cohort, we first performed one-sample MR analyses to identify causal relationships for the 457 observational correlations in the discovery cohort consisting of 1,539 individuals with both metabolic and microbiome traits. We found 58 significant causal effects, of which 17 showed causal effects for gut microbial features on blood metabolic traits and the other 41 showed causal effects for blood metabolic traits on gut microbial features ($P < 1.09 \times 10 = 0.05/457$; Fig. 4 and Supplementary Table 10). Only four of these were bidirectional. By applying one-sample MR analyses to the replication dataset of 1,006 low-depth genomes as well as metabolic and microbiome traits from individuals in different cities, we could replicate 43 of the 58 causal relationships (in the same direction and $P < 0.05$; Supplementary Table 10), indicating that the effects were not random false positives.

Moreover, we also used six different two-sample MR methods, which are more commonly performed when only summary statistics are available from two different cohorts, to analyze our data both in the discovery cohort (summary data for 2,002 samples with metabolic traits and 1,539 samples with microbial features) and the replication cohort (summary data for 1,430 samples with metabolic traits and 1,006 samples with microbial features). The one-sample MR and the two-sample MR analyses showed highly consistent results, and the Spearman's correlation for beta coefficients between one-sample and two-sample MR reached 0.767 for the discovery cohort ($P < 2.2 \times 10^{-16}$). The 58 causal associations identified by one-sample MR were also significant in the two-sample MR analyses. Another 14 causal associations were identified by the two-sample MR analyses (Supplementary Table 11), possibly due to the larger cohort size. We also examined the presence of horizontal pleiotropy by using the MR-PRESSO Global test[18]. Only 1 causal association (the negative effect of selenium on the abundance of *Methylobacillus flagellates*, $P_{\text{MR-PRESSOGlobaltest}} = 0.01$; Supplementary Table 9) showed pleiotropy, while the other 71 causal relationships showed no evidence of pleiotropy ($P > 0.05$). Thus, our MR analyses identified robust causal relationships between blood metabolic traits and specific features of the gut microbiome.

Effects of the gut microbiome on blood metabolic traits. As some of the MR-identified relationships appeared linked, we performed hierarchical clustering for the 12 microbial features and eight blood metabolites involved in the 17 causal relationships from the gut microbiome to blood metabolites, which formed two clusters. One cluster involved decreasing the plasma levels of triglyceride and alanine by gut microbial taxa or functional modules, and the other involved decreasing the levels of 5-methyl THF or progesterone, but increasing serum uric acid or plasma glutamic acid by gut

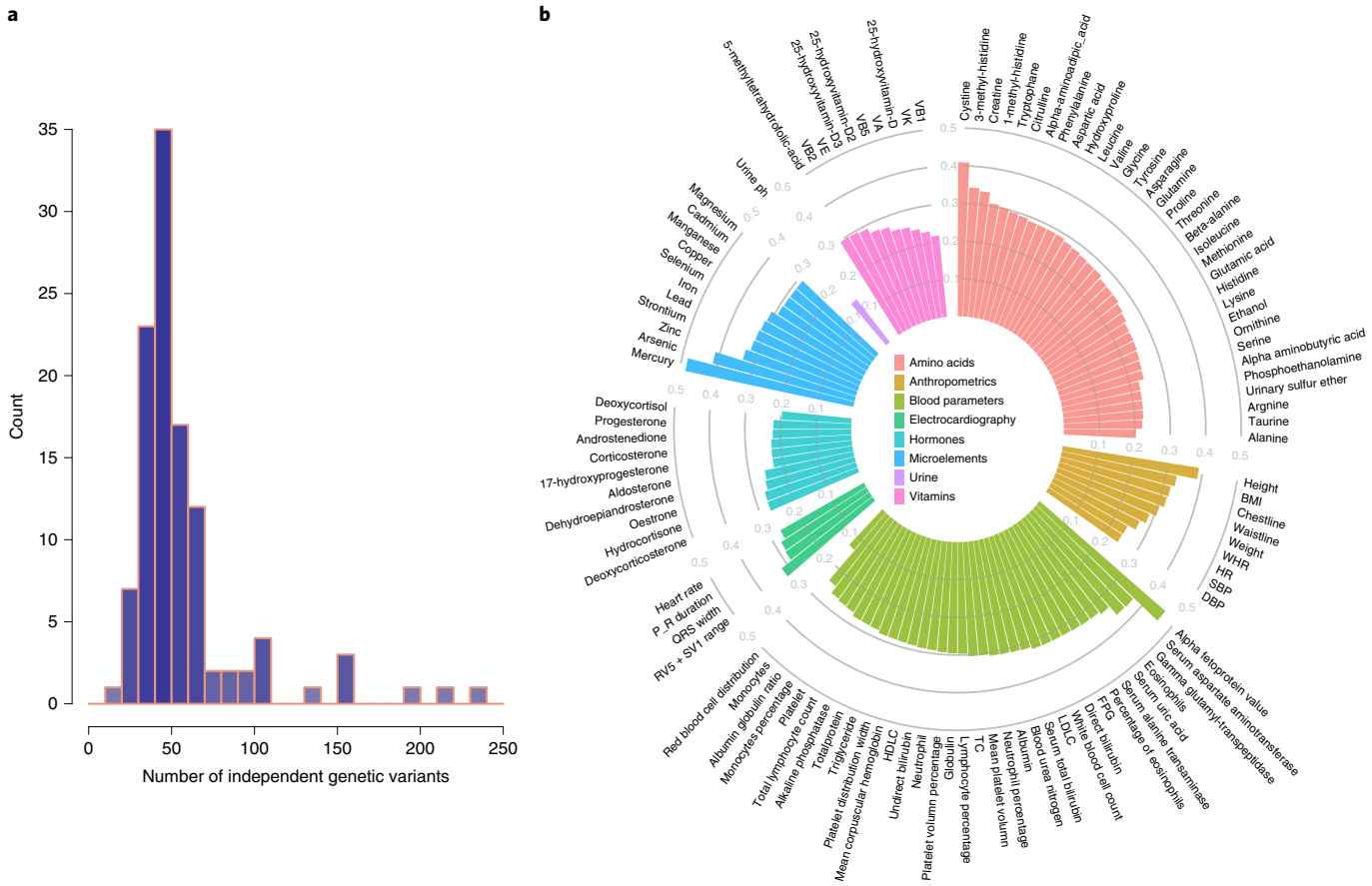

Fig. 3 | Independent genetic variants and their explained variance of metabolic traits. a, Density plot showing the distribution of number of independent genetic variants associated with each metabolic trait ($r^2 < 0.1$ and $P < 1 \times 10^{-5}$), as calculated by GWAS analysis for a total of 112 metabolic traits. The *x* axis indicates the number of independent genetic variants for each metabolic trait. The *y* axis indicates the number of metabolic traits under a given number of independent predictors. **b**, Variance explained by the corresponding independent genetic variants for each metabolic trait. The polar bar plot indicates how much the independent genetic variants of each metabolic trait explained for their phenotypic variance. Each metabolic trait was classified into different catalogs which were marked with different colors. The h^2 was calculated using REML method in GCTA tools.

microbial features (Fig. 4a). Reassuringly, the species *Mobiluncus curtisii* was clustered next to its corresponding genus *Mobiluncus*, and modules including serine degradation and threonine degradation, sucrose degradation and pectin degradation, were likewise next to one another.

The most significant causal effect was *Oscillibacter* on decreasing blood triglyceride concentration (Fig. 5a–c) and, to a lesser extent, on lowering BMI and waist-hip ratio (WHR), whereas the effect with plasma alanine was bidirectional. Using 134 genetic variants to construct a polygenic risk score (PRS) (134 genetic variants and the constructed PRS explained 39.3% and 49.6% of the phenotypic variance, respectively; Fig. 3b and Supplementary Table 10) for one-sample MR analysis in the discovery cohort, we estimated that each 1 s.d. increase in the abundance of *Oscillibacter* would generate a 0.261 mmol l^{-1} decrease in triglyceride concentration ($P = 2.53 \times 10^{-10}$), a 0.161 kg m^{-2} decrease in BMI ($P = 1.33 \times 10^{-4}$) and 0.126 ratio decrease in WHR ($P = 2.73 \times 10^{-3}$). This causal relationship was robust when four two-sample MR tests were performed ($P_{\text{GCTA-GSMR (genome-wide complex trait analysis-generalized summary MR)}} = 4.34 \times 10^{-11}$, $P_{\text{inverse\_variance\_weighted}} = 2.45 \times 10^{-15}$, $P_{\text{weighted-median}} = 1.22 \times 10^{-7}$ and $P_{\text{MR-Egger}} = 1.35 \times 10^{-5}$) (Fig. 5c), and there was no evidence of horizontal pleiotropy ($P_{\text{MR-PRESSOGlobaltest}} = 0.18$; Supplementary Table 11). The reverse MR analysis (testing the effect of genetic predictors of triglyceride on *Oscillibacter* abundance) was significant but did not reach the multiple test corrected significance ($10^{-4} < P < 0.05$). *Oscillibacter* is a Gram-negative Clostridial bacterium, phylogenetically close to *Oscillospira*[19], which can produce valerate or butyrate. In addition, higher relative abundance of *Alistipes* was also associated with decreased blood triglyceride concentration ($P = 8.31 \times 10^{-8}$, Fig. 5d). At the species level, both *Alistipes shahii* ($P = 1.37 \times 10^{-6}$) and *unclassified Alistipes* sp. HGB5 ($P = 3.36 \times 10^{-5}$) showed negative effects on blood triglyceride. The effects of both *Oscillibacter* and *Alistipes* for lowering blood triglyceride concentration were confirmed in the replication cohort ($P = 3.39 \times 10^{-4}$ and $P = 2.88 \times 10^{-4}$, respectively; Supplementary Tables 10 and 11). These findings support the decrease in relative abundances of *Oscillibacter* and *Alistipes* in obese individuals compared with individuals with normal BMI reported in previous studies[20–22], suggesting that these bacteria are promising supplementation agents for individuals of a suitable genetic background.

The gut microbiome potential for pectin degradation II (42.6% of the variance explained by genetic risk score (GRS)) showed a handful of significant MR hits with blood traits (Fig. 4a), including positive effects on alanine ($P = 8.57 \times 10^{-5}$) and serum uric acid ($P = 1.34 \times 10^{-6}$), and negative effects on progesterone ($P = 6.68 \times 10^{-7}$). *Bacteroidetes* and *Fusobacteria* were the only two phyla that positively correlated with the abundance of pectin degradation II (Spearman rank correlation, $\rho = 0.48$ and 0.15, respectively), which included the two previously reported pectin-degrading species *Bacteroides thetaiotaomicron* and *Fusobacterium varium*[23,24].

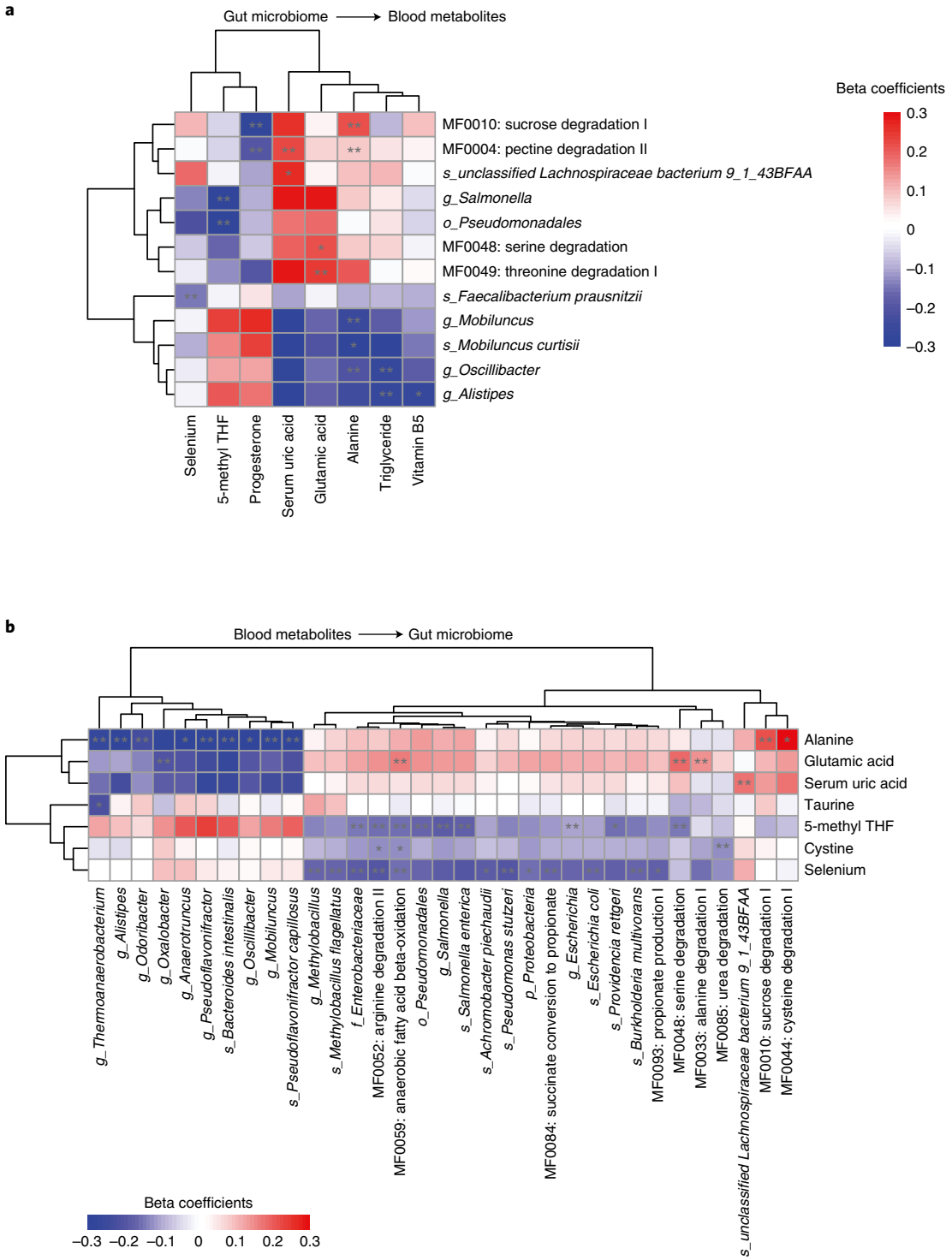

Fig. 4 | Identifying 58 causal relationships for the microbial features and metabolic traits. a, Plot showing the causal effects of 12 specific microbial features on eight metabolic traits involved in the 17 causal associations from gut microbiome to blood metabolites. **b**, Plot showing the causal effects of seven blood metabolites on 33 microbial features involved in 41 causal associations from blood metabolites to gut microbiome. Cells marked with double asterisks represent 43 of the 58 associations identified in the discovery cohort that were also replicated in the replication cohort, while single asterisks represent the other 15 only significant in the discovery cohort. Cells are colored according to the beta coefficients from one-sample MR analysis, with red and blue corresponding to positive and negative associations, respectively.

In the 4D-SZ cohort, *F. varium* correlated with pectin degradation II (Spearman's correlation, $\rho = 0.12$) and increased blood alanine ($P = 0.02$) and serum uric acid ($P = 0.04$); *B. thetaiotaomicron* correlated with pectin degradation II (Spearman's correlation, $\rho = 0.21$) but showed no detectable effect on alanine or uric acid ($P > 0.05$; Supplementary Fig. 7a,b,d). Instead, *Bacteroides dorei*, the bacterial species correlated most strongly with pectin degradation II (Spearman rank correlation, $\rho = 0.32$, Supplementary Fig. 7c), positively

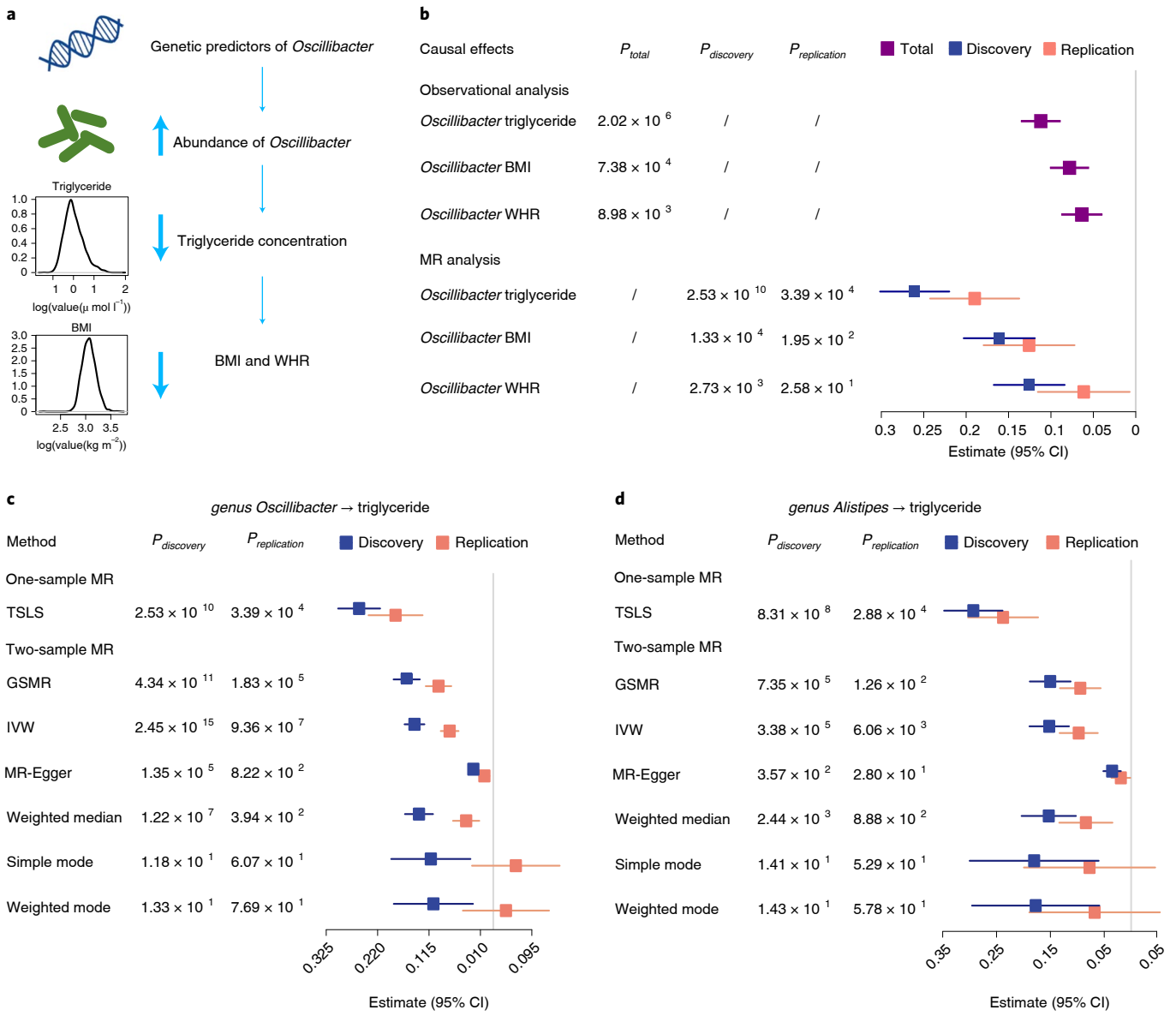

Fig. 5 | Causal effects of genus *Oscillibacter* and *Alistipes* on decreasing blood triglyceride concentration. a, Schematic representation of the MR analysis results: genetic predisposition to higher abundance of *Oscillibacter* is associated with decreased blood triglyceride concentration and, to a lesser extent, for lowering BMI and WHR. **b**, Forest plot representing the effect per 1 s.d. increase in *Oscillibacter* abundance on blood triglyceride, BMI and WHR, as estimated using observational and MR analysis, respectively. Observational correlation analysis was performed using a multivariate linear model in a total of 2,545 samples (purple). One-sample MR analysis was carried out by using a PRS constructed by up to 134 genetic predictors as an instrumental variable, as estimated in the discovery (blue) and replication (red) cohort, respectively. The beta estimates and 95% confidence interval (CI) values as well as *P* values from both the observational and one-sample MR analysis are listed. **c**,**d**, Forest plots representing the MR estimates and 95% CI values of the causal effects of *Oscillibacter* (**c**) and *Alistipes* (**d**) on triglyceride amount, respectively, as estimated using a one-sample MR and six different two-sample MR methods both in the discovery (blue) and replication (red) cohort. The *P* values calculated by each MR method are also listed.

contributed to alanine ($P=0.05$) and serum uric acid levels ($P=3.40\times10^{-4}$; Supplementary Fig. 7d).

Effects of blood metabolites on gut microbial features. For the 41 causal relationships from blood metabolic traits to gut microbial features (one-sample MR; Supplementary Table 10), hierarchical clustering revealed two clusters, one involved mostly decreasing abundance of bacteria by plasma alanine or glutamic acid, and the other decreasing abundance of bacteria by selenium or 5-methyl THF (Fig. 4b). *Faecalibacterium prausnitzii* showed a negative effect on plasma selenium (Fig. 4a), while plasma selenium showed negative effects on gut *Proteobacteria* such as Enterobacteriaceae (for example *Escherichia coli*, $P=3.79\times10^{-5}$), *Pseudomonas stutzeri* ($P=1.06\times10^{-6}$) and modules such as arginine degradation II ($P=2.65\times10^{-6}$), succinate conversion to propionate ($P=3.55\times10^{-5}$) and anaerobic fatty acid beta oxidation ($P=9.71\times10^{-5}$) (Fig. 4b).

Bacteria from the phylum *Proteobacteria* were negatively affected not only by selenium but also by 5-methyl THF (Fig. 4b). We directly verified the effect of 5-methyl THF on *E. coli* in vitro. Supplementing growth media with 5-methyl THF indeed slowed down the growth of *E. coli* strain AM17-9 compared with lower concentrations or absence of 5-methyl THF (Supplementary Fig. 8).

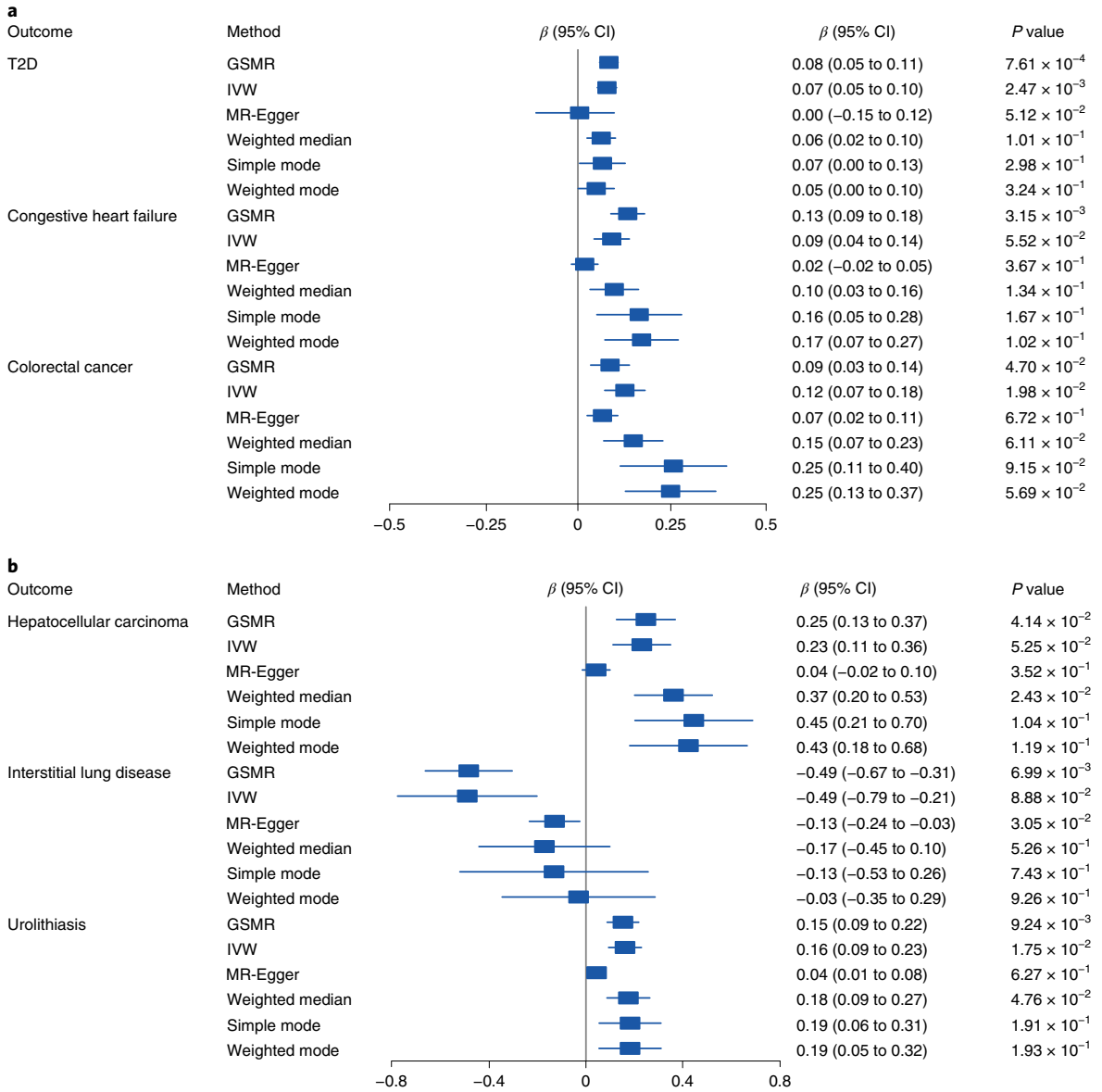

Fig. 6 | Causal effects of *Proteobacteria* and *Escherichia coli* on diseases. a,**b**, Forest plots representing the MR estimates and 95% CI values of the causal effects of *Proteobacteria* (**a**) and *Escherichia coli* (**b**) on diseases, as estimated using six different two-sample MR approaches (GSMR, IVW, MR-Egger, weighted median, simple mode and weighted mode). We show the estimated β values (95% CI) and *P* values, as estimated by each MR approach by using the diseases' summary statistics from Biobank Japan and the gut microbiome GWAS summary data from this discovery cohort with high-depth WGS.

A handful of bacteria were also affected by glutamic acid. The negative influence of glutamic acid (48 variants with suggestive associations and the constructed PRS explained 24.9% and 25.4% of the phenotypic variance, respectively) on the genus *Oxalobacter* ($P=1.56\times10^{-6}$) may help explain the lower prevalence of *Oxalobacter* in developed countries, besides the lower intake of oxalate and antibiotic use[25]. Whether limiting glutamic acid could raise *Oxalobacter* and prevent kidney stones remains to be tested. Glutamic acid negatively affected melibiose degradation (to glucose, galactose, $P=2.05\times10^{-5}$ from two-sample MR), but showed positive effects on alanine degradation I ($P=5.46\times10^{-5}$), anaerobic fatty acid beta oxidation ($P=9.36\times10^{-5}$) and bidirectional positive effect on serine degradation ($P=6.85\times10^{-7}$ for serine degradation to glutamic acid and $P=9.90\times10^{-6}$ for glutamic acid to serine degradation, respectively).

Causal relationships between the gut microbiome and diseases. We further investigated the effects of the 72 significant causal relationships (Supplementary Table 11) involving 40 microbial features and 12 metabolic traits on diseases by performing two-sample MR analysis using gut microbiome GWAS summary data in this 4D-SZ cohort, together with blood quantitative traits and diseases GWAS summary statistics from Biobank Japan[26] (Fig. 1 and Supplementary Table 12), given that Japanese people have a genetic architecture similar to that of Chinese people. Only routine blood parameters but no amino acids, hormones or microelements were included in the Biobank Japan study. Thus, only 5 of the 72 causal associations, involving triglyceride and serum uric acid, were available for further investigation in the Biobank Japan data. The relationship between unclassified Lachnospiraceae bacterium 9_1_43BFAA and uric acid was reciprocal in the 4D-SZ cohort, and we could replicate the

causal effect of uric acid on increased unclassified Lachnospiraceae bacterium 9_1_43BFAA abundance in the Japanese cohort, whereas the reciprocal effect, that is, the potential effect of unclassified Lachnospiraceae bacterium 9_1_43BFAA on uric acid, was not replicated, possibly due to lack of variants in the genotyped Japanese cohort (15 instead of 67; Supplementary Table 13). The other three associations were not replicated, possibly for the same reason. For example, genus *Oscillibacter* had 135 variants with $P<10^{-5}$ in our summary data but only 15 were available in the Biobank Japan summary data.

MR inference using our gut microbiome M-GWAS summary data and disease GWAS summary statistics from Biobank Japan found that *Alistipes*, which showed negative effects on blood triglyceride in the 4D-SZ cohort, lowered the risks of cerebral aneurysm (Supplementary Table 14; $P=4.61\times10^{-4}$) and hepatocellular carcinoma ($P=0.045$) in the Biobank Japan cohort. According to the genetic associations we identified for *Proteobacteria*, we were able to see in Biobank Japan disease data that *Proteobacteria* increased the risk of T2D (Fig. 6a; $P=7.61\times10^{-4}$, two-sample MR), congestive heart failure ($P=0.003$) and colorectal cancer ($P=0.047$). This is consistent with MWAS findings mainly for Enterobacteriaceae[1] and suggest that the metabolites identified above (5-methyl THF, selenium) might help prevent these diseases. Folic acid is indeed recommended for heart disease[27]. In addition, *E. coli* increased the risk of urolithiasis (Fig. 6b; $P=0.009$) and hepatocellular carcinoma ($P=0.04$) but decreased interstitial lung disease risk ($P=0.007$). Similarly, *Salmonella enterica* increased prostate cancer risk but decreased interstitial lung disease risk. The order Pseudomonadales was the only microbial feature showing a positive effect on pulmonary tuberculosis. The denitrifying bacteria *Achromobacter* increased the risk of atopic dermatitis ($P=0.005$), gastric cancer ($P=0.008$), esophageal cancer ($P=0.027$) and biliary tract cancer ($P=0.034$). *Bacteroides intestinalis*, which was reported to be relatively depleted in patients of atherosclerotic cardiovascular disease[28], was found here to increase with potassium, and *B. intestinalis* showed a negative effect on epilepsy. *Streptococcus parasanguinis* had a positive effect on colorectal cancer and posterior wall thickness (echocardiography), consistent with MWAS studies[1,28,29]. These results illustrate the potential significance of gut microbiome–blood metabolite relationships in understanding and preventing cardiometabolic diseases and cancer.

Discussion

We identified many genetic loci associated with microbial features and metabolic traits, and found 58 causal relationships between the gut microbiome and blood metabolites using one-sample BMR. Out of the 58 one-sample MR signals, 43 could be replicated in a low-depth genome sequenced cohort also from China. Two-sample MR replicated the 58 causal relationships in the same direction and identified another 14 causal relationships. Two-sample MR using summary statistics from Biobank Japan identified effects of gut microbial features on diseases, suggesting potential applications of microbiome intervention in cardiometabolic, kidney and lung diseases, and cancer. While mechanistic investigations using germ-free mice and reference bacterial strains have been popular, our data-driven analyses underscore the clinical relevance of gut microbes that have not been cultured and characterized extensively, for example *Oscilibacter* and *Alistipes*, for lowering triglyceride concentration and a number of disease risks, which may be particularly relevant for East Asian regions undergoing rapid changes in lifestyle and disease profiles.

Although associations between the gut microbiome and blood features such as amino acids and vitamins have been known for some time, our MR analyses could inspire more mechanistic and interventional studies. The unique data available from the 4D-SZ cohort allowed appreciation of overlooked features such as selenium. Interestingly, while selenium showed adverse effects on Gammaproteobacteria, *F. prausnitzii* showed a negative effect on plasma selenium. Nitrogen is a limiting resource for many ecosystems. In the modern human gut microbiome, without high intake of nitrite, proteins are probably the main source of nitrogen[30], and the glutamate–glutamine reservoir is a key buffering mechanism for the inflammatory potential of excess amines[31–34]. The increase in *Proteobacteria* and decrease in Oxalobacteraceae observed in these Chinese individuals (no more than 30 years old on average) could potentially explain susceptibility to cardiometabolic and kidney diseases later in life. The bidirectional link between strontium and *Streptococcus parasanguinis* implies an interplay between water source and cardiovascular diseases[28,35].

Metabolism of polysaccharides that cannot be digested directly by the host is an important function of the colonic microbiome. We found degradation of pectin (or sucrose) to negatively affect progesterone level. This is an interesting possibility to provide scientific support for traditional dietary advice for pregnant women to ensure full-term pregnancy. Hyperuricemia and gout is a growing epidemic in East Asia, and soft drinks containing fructose are a strong factor that is no less important than beer and meat[36]. Gut microbial (*Bacteroides*, *Fusobacterium*) pectin degradation module contributed positively to circulating levels of alanine and uric acid. Further studies on the transkingdom metabolic flux of carbon and nitrogen would be necessary for personalized management of uric acid and alanine levels.

For the nascent field of M-GWAS and microbiome MR, there are also a lot of opportunities for methodological development by statistical experts. Low-frequency microbes are common in an individual's gut and could play physiological or pathological roles[1,37]. Our MR results for gut microbial species were supported by MR for higher taxonomic units such as genus or phylum (Fig. 4 and Supplementary Table 11). Yet, the *P* values were sometimes more significant for the larger taxa, suggesting similar functions contributed by other species. Functional redundancy in the microbiome has been discussed ever since the beginning of the microbiome field[38,39], and here we identified study-wide significant host genetic associations with gut microbial functional modules, and causal effects of other gut microbial functional modules on host levels of circulating metabolites. Distribution of the microbiome taxonomic or functional data constitutes another layer of consideration, in addition to the human allele frequencies. Gathering a more homogenous cohort could enable identification of signals in a relatively small cohort, while corrections for comparing different populations might involve host–microbiome interactions. As the gut microbiome can be influenced by medication[40], and heritability for most traits is higher in younger individuals[41], healthy young adults are probably preferable for M-GWAS studies, while microbiome–drug interactions in older individuals could be an important direction for MR studies.

Overall, our data-driven approach underscores the great potential of M-GWAS and MR for a full picture of the microbiome, which can be mechanistically illuminating and are poised to help focus intervention efforts to mitigate inflammation and prevent or alleviate complex diseases.

Online content

Any methods, additional references, Nature Research reporting summaries, source data, extended data, supplementary information, acknowledgements, peer review information; details of author contributions and competing interests; and statements of data and code availability are available at https://doi.org/10.1038/s41588-021-00968-y.

Received: 23 January 2020; Accepted: 14 October 2021;
Published online: 3 January 2022

References

1. Wang, J. & Jia, H. Metagenome-wide association studies: fine-mining the microbiome. *Nat. Rev. Microbiol.* **14**, 508–522 (2016).
2. Moschen, A. R. et al. Lipocalin 2 protects from inflammation and tumorigenesis associated with gut microbiota alterations. *Cell Host Microbe* **19**, 455–469 (2016).
3. Long, X. et al. *Peptostreptococcus anaerobius* promotes colorectal carcinogenesis and modulates tumour immunity. *Nat. Microbiol.* **4**, 2319–2330 (2019).
4. Zhu, F. et al. Transplantation of microbiota from drug-free patients with schizophrenia causes schizophrenia-like abnormal behaviors and dysregulated kynurenine metabolism in mice. *Mol. Psychiatry* **25**, 2905–2918 (2020).
5. Liu, X. et al. A genome-wide association study for gut metagenome in Chinese adults illuminates complex diseases. *Cell Discov.* **7**, 9 (2021).
6. Bonder, M. J. et al. The effect of host genetics on the gut microbiome. *Nat. Genet.* **48**, 1407–1412 (2016).
7. Wang, J. et al. Genome-wide association analysis identifies variation in vitamin D receptor and other host factors influencing the gut microbiota. *Nat. Genet.* **48**, 1396–1406 (2016).
8. Turpin, W. et al. Association of host genome with intestinal microbial composition in a large healthy cohort. *Nat. Genet.* **48**, 1413–1417 (2016).
9. Blekhman, R. et al. Host genetic variation impacts microbiome composition across human body sites. *Genome Biol.* **16**, 191 (2015).
10. Rothschild, D. et al. Environment dominates over host genetics in shaping human gut microbiota. *Nature* **555**, 210–215 (2018).
11. Burgess, S., Timpson, N. J., Ebrahim, S. & Davey Smith, G. Mendelian randomization: where are we now and where are we going? *Int. J. Epidemiol.* **44**, 379–388 (2015).
12. Yang, Q., Lin, S. L., Kwok, M. K., Leung, G. M. & Schooling, C. M. The roles of 27 genera of human gut microbiota in ischemic heart disease, type 2 diabetes mellitus, and their risk factors: a Mendelian randomization study. *Am. J. Epidemiol.* **187**, 1916–1922 (2018).
13. Sanna, S. et al. Causal relationships among the gut microbiome, short-chain fatty acids and metabolic diseases. *Nat. Genet.* **51**, 600–605 (2019).
14. Sakaue, S. et al. Trans-biobank analysis with 676,000 individuals elucidates the association of polygenic risk scores of complex traits with human lifespan. *Nat. Med.* **26**, 542–548 (2020).
15. Shin, S. Y. et al. An atlas of genetic influences on human blood metabolites. *Nat. Genet.* **46**, 543–550 (2014).
16. Cox, A. J. et al. Association of SNPs in the *UGT1A* gene cluster with total bilirubin and mortality in the Diabetes Heart Study. *Atherosclerosis* **229**, 155–160 (2013).
17. MacArthur, J. et al. The new NHGRI-EBI Catalog of published genome-wide association studies (GWAS Catalog). *Nucleic Acids Res.* **45**, D896–D901 (2017).
18. Verbanck, M., Chen, C. Y., Neale, B. & Do, R. Detection of widespread horizontal pleiotropy in causal relationships inferred from Mendelian randomization between complex traits and diseases. *Nat. Genet.* **50**, 693–698 (2018).
19. Katano, Y. et al. Complete genome sequence of *Oscillibacter valericigenes* Sjm18-20^{T} (=NBRC 101213^{T}). *Stand. Genom. Sci.* **6**, 406–414 (2012).
20. Thingholm, L. B. et al. Obese individuals with and without type 2 diabetes show different gut microbial functional capacity and composition. *Cell Host Microbe* **26**, 252–264.e10 (2019).
21. Hu, H. J. et al. Obesity alters the microbial community profile in Korean adolescents. *PLoS One* **10**, e0134333 (2015).
22. Tims, S. et al. Microbiota conservation and BMI signatures in adult monozygotic twins. *ISME J.* **7**, 707–717 (2013).
23. Noack, J., Dongowski, G., Hartmann, L. & Blaut, M. The human gut bacteria *Bacteroides thetaiotaomicron* and *Fusobacterium varium* produce putrescine and spermidine in cecum of pectin-fed gnotobiotic rats. *J. Nutr.* **130**, 1225–1231 (2000).
24. Luis, A. S. et al. Dietary pectic glycans are degraded by coordinated enzyme pathways in human colonic Bacteroides. *Nat. Microbiol.* **3**, 210–219 (2018).
25. PeBenito, A. et al. Comparative prevalence of *Oxalobacter formigenes* in three human populations. *Sci. Rep.* **9**, 574 (2019).
26. Ishigaki, K. et al. Large-scale genome-wide association study in a Japanese population identifies novel susceptibility loci across different diseases. *Nat. Genet.* **52**, 669–679 (2020).
27. Huo, Y. et al. Efficacy of folic acid therapy in primary prevention of stroke among adults with hypertension in China: the CSPPT randomized clinical trial. *JAMA* **313**, 1325–1335 (2015).
28. Jie, Z. et al. The gut microbiome in atherosclerotic cardiovascular disease. *Nat. Commun.* **8**, 845 (2017).
29. Yachida, S. et al. Metagenomic and metabolomic analyses reveal distinct stage-specific phenotypes of the gut microbiota in colorectal cancer. *Nat. Med.* **25**, 968–976 (2019).
30. Reese, A. T. et al. Microbial nitrogen limitation in the mammalian large intestine. *Nat. Microbiol.* **3**, 1441–1450 (2018).
31. Petrus, P. et al. Glutamine links obesity to inflammation in human white adipose tissue. *Cell Metab.* **31**, 375–390.e11 (2019).
32. Liu, R. et al. Gut microbiome and serum metabolome alterations in obesity and after weight-loss intervention. *Nat. Med.* **23**, 859–868 (2017).
33. Choi, W. M. et al. Glutamate signaling in hepatic stellate cells drives alcoholic steatosis. *Cell Metab.* **30**, 877–889.e877 (2019).
34. Kang, D. J. et al. Gut microbiota drive the development of neuroinflammatory response in cirrhosis in mice. *Hepatology* **64**, 1232–1248 (2016).
35. Long, T. et al. Plasma metals and cardiovascular disease in patients with type 2 diabetes. *Environ. Int.* **129**, 497–506 (2019).
36. Kuo, C. F., Grainge, M. J., Zhang, W. & Doherty, M. Global epidemiology of gout: prevalence, incidence and risk factors. *Nat. Rev. Rheumatol.* **11**, 649–662 (2015).
37. Li, J. et al. An integrated catalog of reference genes in the human gut microbiome. *Nat. Biotechnol.* **32**, 834–841 (2014).
38. Qin, J. et al. A human gut microbial gene catalogue established by metagenomic sequencing. *Nature* **464**, 59–65 (2010).
39. Human Microbiome Project Consortium. Structure, function and diversity of the healthy human microbiome. *Nature* **486**, 207–214 (2012).
40. Maier, L. et al. Extensive impact of non-antibiotic drugs on human gut bacteria. *Nature* **555**, 623–628 (2018).
41. Polderman, T. J. et al. Meta-analysis of the heritability of human traits based on fifty years of twin studies. *Nat. Genet.* **47**, 702–709 (2015).
42. Yang, J., Lee, S. H., Goddard, M. E. & Visscher, P. M. GCTA: a tool for genome-wide complex trait analysis. *Am. J. Hum. Genet.* **88**, 76–82 (2011).

Methods

Study participants. All adult Chinese individuals included in this study were recruited for a multiomic study, with some volunteers having samples from as early as 2015, which would constitute the time dimension in '4D'. The discovery cohort was recruited during a physical examination from March to May in 2017 in the city of Shenzhen, including 2,002 individuals with blood samples, of which 1,539 had fecal samples. All these individuals were enlisted for high-depth whole-genome and whole-metagenomic sequencing. For replication, blood samples were collected from 1,430 individuals, of which 1,006 had fecal samples. The replication cohort was designed in the same manner but organized at smaller scales in multiple cities (Wuhan, Qingdao, etc.) in China. The protocols for blood and stool collection, as well as the whole-genome and metagenomic sequencing, were similar to our previous studies[5,43–45]. For blood samples, buffy coat was isolated and DNA extracted using HiPure Blood DNA Mini Kit (Magen, catalog no. D3111) according to the manufacturer's protocol. Feces were collected with an MGIEasy kit, and stool DNA was extracted in accordance with the MetaHIT protocol as described previously[5,42]. The DNA concentrations from blood and stool samples were estimated by Qubit (Invitrogen). Input DNA (200 ng) from blood and stool samples were used for library preparation and then processed for paired-end 100-bp and single-end 100-bp sequencing, respectively, using a BGISEQ-500 platform[46].

The study was approved by the Institutional Review Boards (IRB) at BGI-Shenzhen, and all participants provided written informed consent at enrollment.

High-depth whole-genome sequence for the discovery cohort. A total of 2,002 individuals in the discovery cohort were sequenced to a mean sequencing depth of 42× for the whole genome. The reads were aligned to the latest reference human genome GRCh38/hg38 with BWA[47] (v.0.7.15) with default parameters. The reads consisting of base quality less than five or containing adapter sequences were filtered out. The alignments were indexed in the BAM format using Samtools[48] (v.0.1.18) and PCR duplicates were marked for downstream filtering using Picardtools (v.1.62). The Genome Analysis Toolkit's (GATK[49], v.3.8) BaseRecalibrator created recalibration tables to screen known SNPs and insertions or deletions (INDELs) in the BAM files from dbSNP (v.150). GATKlite (v.2.2.15) was used for subsequent base quality recalibration and removal of read pairs with improperly aligned segments as determined by Stampy. GATK's HaplotypeCaller were used for variant discovery. GVCFs containing SNVs and INDELs from GATK HaplotypeCaller were combined (CombineGVCFs), genotyped (GenotypeGVCFs), variant score recalibrated (VariantRecalibrator) and filtered (ApplyRecalibration). During the GATK VariantRecalibrator process, we took our variants as inputs and used four standard SNP sets to train the model: (1) HapMap3.3 SNPs; (2) dbSNP build 150 SNPs; (3) 1000 Genomes Project SNPs from Omni 2.5 chip and (4) 1000 G phase1 high confidence SNPs. The sensitivity threshold of 99.9% to SNPs and 99% to INDELs were applied for variant selection after optimizing for Transition to Transversion (TiTv) ratios using the GATK ApplyRecalibration command. After applying the recalibration, there were 60,978,451 raw variants left, including 55 million SNPs, and 6 million INDELs.

We applied a conservative inclusion threshold for variants: (1) mean depth >8×; (2) Hardy-Weinberg equilibrium (HWE) $P > 10^{-5}$ and (3) genotype calling rate >98%. We required samples to meet these criteria: (1) mean sequencing depth >20×; (2) variant calling rate > 98%; (3) no population stratification by performing principal components analysis (PCA) analysis implemented in PLINK[50] (v.1.9) and (4) excluding related individuals by calculating pairwise identity by descent (IBD, Pi-hat threshold of 0.1875) in PLINK. Only ten samples were removed in quality control filtering. After variant and sample quality control, 1,992 individuals with 6.12 million common (MAF ≥ 5%) and 3.90 million low-frequency (0.5% ≤ MAF < 5%) variants from the discovery cohort were left for subsequent analyses.

Low-depth whole-genome sequence for the replication cohort. A total of 1,430 individuals in the replication cohort were sequenced to a mean sequencing depth of 8× for the whole genome. We used BWA to align the whole-genome reads to GRCh38/hg38, and GATK to perform variant calling by applying the same pipelines as for the high-depth WGS data. After completing the joint calling process with CombineGVCFs and GenotypeGVCFs options, we obtained 43,402,368 raw variants. A more stringent process in the GATK VariantRecalibrator stage compared with the high-depth WGS was then used, and the sensitivity threshold of 98.0% to both SNPs and INDELs was applied for variant selection after optimizing for TiTv ratios using the GATK ApplyRecalibration command. Further, we kept variants with <10% missing genotype frequency and minor allele count greater than five. All these high-quality variants were then imputed using BEAGLE 5 (ref. [51]) with the 1,992 high-depth WGS dataset as reference panel. We retained only variants with imputation information >0.7 and obtained 10,905,418 imputed variants. We further filtered this dataset to keep variants with HWE $P > 10^{-5}$ and genotype calling rate > 90%. Similar to what we did for the discovery cohort, samples were required to have mean sequencing depth >6×, variant call rate >98%, no population stratification and no kinship. Finally, 1,430 individuals with 5,884,439 high-quality common and low-frequency variants (MAF ≥ 0.5%) from the replication cohort were left for subsequent analysis. To assess the data quality, we sequenced 27 samples with both high-depth and low-depth WGS data and then compared the 5,318,809 variants between them for each individual. The average genotype concordance was 98.66% (Supplementary Table 15).

Metagenomic sequencing and profiling. We performed high-quality whole-metagenomic sequencing for 1,539 samples from the discovery cohort and 1,004 samples from the replication cohort with fecal samples available. The reads were aligned to hg38 using SOAP2 (ref. [52]) (v.2.22; identity ≥0.9) to remove human reads. The gene profiles were generated by aligning high-quality sequencing reads to the integrated gene catalog (IGC) by using SOAP2 (identity ≥0.95) as previously described[37]. The relative abundance profiles of phylum, order, family, class, genera and species were determined from the gene abundances. To eliminate the influence of sequencing depth in comparative analyses, we downsized the unique IGC mapped reads to 20 million for each sample. The relative abundance profiles of gene, phylum, order, family, class, genus and species were determined accordingly using the downsized mapped reads per sample.

Gut metabolic modules (GMMs) reflect bacterial and archaeal metabolism specific to the human gut, with a focus on anaerobic fermentation processes[53]. The current set of GMMs was built through an extensive review of the literature and metabolic databases, inclusive of MetaCyc[54] and KEGG, followed by expert curation and delineation of modules and alternative pathways. Finally, we identified 620 common microbial taxa and GMMs present in 50% or more of the samples.

Metabolic trait profiling. Measurements of metabolic traits (anthropometric characteristics and blood metabolites) were performed for all 3,432 individuals during the physical examination in this study. The clinical tests, including blood tests and urinalysis, were performed by a licensed physical examination organization. Anthropometric measurements such as height, weight, waistline and hipline were measured by nurses. Age and gender were self-reported. The metabolites, that is, vitamins, hormones, amino acids and trace elements including heavy metals, were chosen from a health management perspective. Measurements of blood metabolites were performed as described in detail by Jie et al.[39]; blood amino acids were measured by ultra high pressure liquid chromatography (UHPLC) coupled to a Qtrap 5500 mass spectrometry (AB Sciex) with the electrospray ionization (ESI) source in positive ion mode using 40 µl plasma; blood hormones were measured by UHPLC coupled to an AB Sciex Qtrap 5500 mass spectrometry with the atmospheric pressure chemical ionization (APCI) source in positive ion mode using 250 µl plasma; blood trace elements were measured by an 7700x ICP-MS (Agilent Technologies) equipped with an octupole reaction system (ORS) collision/reaction cell technology to minimize spectral interferences using 200 µl whole blood; water-soluble vitamins were measured by UPLC coupled to a Xevo TQ-S Triple Quad mass spectrometry (Waters) with the ESI source in positive ion mode using 200 µl plasma; fat-soluble vitamins were measured by UPLC coupled to an AB Sciex Qtrap 4500 mass spectrometry with the APCI source in positive ion mode using 250 µl plasma.

Observational correlation analyses. As many microbial features (taxonomies and pathways) are highly correlated, we first performed a number of Spearman correlation tests and kept only one member of pairs of bacteria or GMMs showing >0.99 correlation coefficient. This filtering resulted in a final set of 500 unique features (99 GMMs and 401 gut taxa) that were used for analyses. We correlated these 500 microbial features with 112 measured metabolic traits, including nine anthropometric measurements (BMI, WHR, etc.) and 103 blood metabolites (amino acids, vitamins, microelements, etc.) in the 3,432 individuals. All metabolic traits and microbial features were transformed using natural logarithmic function to reduce skewness of distributions. For each phenotype, we excluded outlier individuals with more than 4 s.d. away from the mean. The metabolite measures were then centered and scaled to mean of zero and s.d. =1.

The relationship between metabolic traits and microbial features were evaluated by multivariable linear regression analysis while adjusted for age and gender. After achieving the raw *P* value, we used the *p.adjust()* function in R (v.3.2.5) to perform the multiple test correction and calculated adjusted *P* values with the Benjamini–Hochberg procedure. The results were considered significant when the FDR-adjusted *P* value was <0.05. The correlated microbial features and metabolic traits, raw *P* and FDR-adjusted *P* values are included in Supplementary Table 9.

Clustering of microbiome–metabolite associations. To assess the association clusters of 58 identified causal relationships involving the effects of 12 microbial features on eight metabolic traits and the effects of seven metabolic traits on 33 microbial features, we performed a hierarchical clustering analysis. Beta coefficients of associations between the microbial features and metabolic traits from one-sample MR analysis were used to construct distance matrices. Complete-linkage hierarchical clustering was used to cluster the metabolites and microbiome traits from the distance matrices using the 'hclust' function in R, and the results were visualized as a heatmap.

Genome-wide association analysis for microbial features. We tested the associations between host genetic variants and gut bacteria using a linear or logistic model based on the abundance of gut bacteria. The abundance of bacteria with occurrence rate over 95% in the cohort was transformed by the natural logarithm and any outlier individual located away from the mean by more than 4 s.d. was removed, so that the abundance of bacteria could be treated as a quantitative trait. Otherwise, we dichotomized bacteria into presence/absence patterns to prevent zero inflation; the abundance of bacteria could then be treated as a dichotomous trait. Next, for 10 million common and low-frequency variants (0.5% ≤ MAF < 5%) identified in the discovery cohort and 5.9 million common and low-frequency variants identified in replication cohort, we performed a standard single variant (SNP/INDEL)-based M-GWAS analysis via PLINK using a linear model for quantitative trait or a logistic model for dichotomous trait. Given the effects of diet and lifestyles on microbial features, we included age, gender, BMI, defecation frequency, stool form and 12 diet and lifestyle factors, as well as the top four PCs as covariates for M-GWAS analysis in both the discovery and the replication cohort.

Genome-wide association analysis for metabolic traits. For each of the 112 anthropometric and metabolic traits, the $\log_{10}$-transformed median-normalized values were used as a quantitative traits. Samples with missing values and values beyond 4 s.d. from the mean were excluded from association analysis. Each of the 10 million common and low-frequency variants identified in the discovery cohort and the 5.9 million common and low-frequency variants identified in the replication cohort was tested independently using a linear model for quantitative trait implemented in PLINK. Age, gender and the top four PCs were included as covariates.

Independent predictor and explained phenotypic variance. For each whole-genome-wide association result of microbial features and metabolic traits, we first selected genetic variants that showed association at $P < 1 \times 10^{-5}$ and then performed a linkage disequilibrium (LD) estimation with a threshold of LD $r^2 < 0.1$ for clumping analysis to obtain independent genetic predictors. The P value threshold of 1×10^{-5} was used for selection of genetic predictors associated with microbial features by maximizing the strength of genetic instruments and the amount of the average genetic variance explained by the genetic predictors in an independent sample. For each microbial feature, we got genetic instruments in discovery cohort using different P thresholds, including 5×10^{-8}, 1×10^{-7}, 1×10^{-6} and 1×10^{-5}. We tested the strength of these instruments under different P thresholds by checking whether they predicted corresponding microbial features in an independent sample (Supplementary Note, Supplementary Table 16 and Supplementary Fig. 6), and we observed that the mean value of instrumental F statistics is 3.57 and, on average, only 0.28% phenotype variance could be explained by instruments on microbial features when using 5×10^{-8} as instrumental cut-off. Therefore, we used a more liberal threshold of $P < 1 \times 10^{-5}$ to select the instruments for microbial features, and the instrumental mean F statistics reached 51.4 (>10), which indicates a strong instrument[55]. The average phenotypic variance explained by instruments on microbial features was 22.6% for the discovery cohort and 5.09% for the replication cohort (Supplementary Fig. 2). For consistency, we used the same threshold and procedure for selecting genetic predictors of metabolic traits in both the discovery and the replication cohort. The LD estimation between variants was calculated in 2,002 samples for the discovery cohort and in 1,430 samples for the replication cohort, respectively. For each phenotype, the variance explained by the corresponding independent genetic predictors was estimated using a restricted maximum likelihood (REML) model as implemented in the GCTA software[55]. We adjusted for age, gender and the top four PCs in the REML analysis.

One-sample MR analysis. To investigate the causal effects between microbial features and metabolic traits available from the same cohort, we first performed one-sample BMR analysis in the discovery cohort, which included 1,539 individuals with both metabolite and microbiome traits. We specified a threshold of $P < 1 \times 10^{-5}$ to select SNP instruments and LD $r^2 < 0.1$ threshold for clumping analysis to get independent genetic variants for MR analysis. Then, an unweighted PRS was calculated for each individual using independent genetic variants from GWAS data. Each SNP was recoded as 0, 1 and 2, depending on the number of trait-specific risk increasing alleles carried by an individual. We performed instrumental variable (IV) analyses employing the two-stage least square regression (TSLS) method[56]. In the first stage, for each exposure trait, association between the GRS and observational phenotype value was assessed using linear regression and predicted fitted values based on the instrument were obtained. In the second stage, we performed linear regression with outcome trait and genetically predicted exposure level from the first stage. In both stages, analyses were adjusted for age, gender and the top four PCs of population structure. For each trait, we performed TSLS using the 'ivreg' command from the AER package in R. We attempted to replicate the causal effects between traits in replication cohort with 1,004 individuals.

Two-sample MR analysis. To maximize the sample size in MR analysis and confirm the causal effects between microbial features and metabolic traits, we also performed two-sample BMR analysis using six different methods, including a GCTA-GSMR approach[57] and five other methods (inverse-variance weighting (IVW)[58,59], MR-Egger regression[60,61], weighted median[62], mode-based estimate (MBE)[63] including Simple mode and Weighted mode) implemented in the "TwoSampleMR" R package as a robust validation. A consistent effect across the six methods is less likely to be a false positive. If the genetic variants have horizontally pleiotropic effects but are independent of the effects of the genetic variants upon exposure, this is known as balanced pleiotropy. If all the pleiotropic effects are biasing the estimate in the same direction (directional pleiotropy), this will bias the results (with the exception of the MR-Egger method). We used the MR pleiotropy residual sum and outlier (MR-PRESSO) global test to estimate for the presence of directional pleiotropy.

We first performed GWAS analysis for every trait and then used summary statistics data for two-sample MR analysis. Genetic variants with $P < 1 \times 10^{-5}$ and LD $r^2 < 0.1$ were selected as instrumental variables.

In vitro growth experiments of *E. coli*. To directly test the interactions between *E. coli* and 5-methyl THF, the anaerobic growth of *E. coli* strain AM17-9 was characterized at different concentrations of 5-methyl THF. *E. coli* strain AM17-9, isolated from feces of a male, was grown routinely in Luria-Bertani (LB) broth while supplementing 5-methyl THF with concentrations of 0, 1 and 2 ng ml^{-1}, respectively. The normal concentration of 5-methyl THF in human blood ranges from 4.4 ng ml^{-1} to 32.8 ng ml^{-1}. The growth of *E. coli* AM17-9 was inhibited when supplementing 5-methyl THF from 0 to 2 ng ml^{-1}. The optical density at 600 nm was measured at intervals of 2 h using a microplate reader.

MR analyses for diseases in Biobank Japan. We downloaded summary statistics data for 42 diseases and 59 blood quantitative traits in 212,453 Japanese individuals[26] (http://jenger.riken.jp/en/result; Supplementary Table 13). By combining these data and the gut microbiome GWAS summary data from the discovery cohort with high-depth WGS, we performed a two-sample BMR analysis to investigate the causal effect between exposure (40 microbial features and 12 metabolic traits involved in 72 significant causal relationships; Fig. 4) and outcome (42 diseases from BioBank Japan) by applying the GSMR method and the other five MR tests described above. For consistency, genetic variants with $P < 1 \times 10^{-5}$ and LD $r^2 < 0.1$ were also selected as instrumental variables for phenotypes in the Biobank Japan study.

Reporting Summary. Further information on research design is available in the Nature Research Reporting Summary linked to this article.

Data availability

The human reference hg38 datasets are publicly available from http://hgdownload.soe.ucsc.edu/goldenPath/hg38/bigZips/. All summary statistics that support the findings of this study, including the associations between host genetics and microbiomes, host genetics and metabolites are publicly available from https://ftp.cngb.org/pub/CNSA/data2/CNP0000794/. The release of the data was approved by the Ministry of Science and Technology of China (Project ID: 2020BAT1137). Individual-level data including host genetics, metagenomics and metabolites have been uploaded to the GSA database (https://ngdc.cncb.ac.cn/bioproject/browse/PRJCA005334). Access to individual-level data has to be approved by corresponding authors (tao.zhang@genomics.cn, jiahuijue@genomics.cn), and is subject to the policies and approvals from the Human Genetic Resource Administration, Ministry of Science and Technology of the People's Republic of China. The summary statistics data for 42 diseases and 59 blood quantitative traits in 212,453 Japanese individuals are available from Biobank Japan (http://jenger.riken.jp/en/result).

Code availability

The host genome reads were aligned to the latest reference human genome GRCh38/hg38 with BWA (v.0.7.15; http://bio-bwa.sourceforge.net/). The alignments were indexed in the BAM format using Samtools (v.0.1.18; http://samtools.sourceforge.net/) and PCR duplicates were marked for downstream filtering using Picardtools (v.1.62; http://broadinstitute.github.io/picard/). The genome variants calling were performed using GATK (v.3.8; https://gatk.broadinstitute.org/hc/en-us). The low-depth data were imputed using BEAGLE (v.5.0; https://faculty.washington.edu/browning/beagle/b5_0.html). The metagenome reads were aligned to hg38 using SOAP (v.2.22; http://soap.genomics.org.cn). Quality control, association analyses and GRS analyses were performed in PLINK (v.1.90; http://zzz.bwh.harvard.edu/plink/). We performed variance explained analysis using the REML model in GCTA (v.1.26.0; https://cnsgenomics.com/software/gcta) and one-sample MR analyses using the TSLS method in the AER package (v.1.2-9; https://www.rdocumentation.org/packages/AER/versions/1.2-9/topics/ivreg). Two-sample MR analyses were performed in GSMR (v.1.0.7; http://cnsgenomics.com/software/gsmr/) and TwoSampleMR (v.0.5.6; https://mrcieu.github.io/TwoSampleMR/). All statistics analyses and visualizations were performed in R (v.3.2.5; https://www.r-project.org).

References

43. Jie, Z. et al. A transomic cohort as a reference point for promoting a healthy human gut microbiome. *Med. Microecol.* **8**, 100039 (2021).
44. Zhu, J. *et al*. Over 50,000 metagenomically assembled draft genomes for the human oral microbiome reveal new taxa. *Genomics Proteom. Bioinform.* https://doi.org/10.1016/j.gpb.2021.05.001 (2021).
45. Liu, X. *et al*. Metagenome-genome-wide association studies reveal human genetic impact on the oral microbiome. Preprint at *bioRxiv* https://doi.org/10.1101/2021.05.06.443017 (2021).
46. Fang, C. et al. Assessment of the cPAS-based BGISEQ-500 platform for metagenomic sequencing. *Gigascience* **7**, 1–8 (2018).
47. Li, H. & Durbin, R. Fast and accurate short read alignment with Burrows-Wheeler transform. *Bioinformatics* **25**, 1754–1760 (2009).
48. Li, H. et al. The Sequence Alignment/Map format and SAMtools. *Bioinformatics* **25**, 2078–2079 (2009).
49. McKenna, A. et al. The Genome Analysis Toolkit: a MapReduce framework for analyzing next-generation DNA sequencing data. *Genome Res.* **20**, 1297–1303 (2010).
50. Purcell, S. et al. PLINK: a tool set for whole-genome association and population-based linkage analyses. *Am. J. Hum. Genet.* **81**, 559–575 (2007).
51. Browning, B. L., Zhou, Y. & Browning, S. R. A one-penny imputed genome from next-generation reference panels. *Am. J. Hum. Genet.* **103**, 338–348 (2018).
52. Li, R. et al. SOAP2: an improved ultrafast tool for short read alignment. *Bioinformatics* **25**, 1966–1967 (2009).
53. Vieira-Silva, S. et al. Species-function relationships shape ecological properties of the human gut microbiome. *Nat. Microbiol.* **1**, 16088 (2016).
54. Caspi, R. et al. The MetaCyc database of metabolic pathways and enzymes and the BioCyc collection of Pathway/Genome Databases. *Nucleic Acids Res.* **42**, D459–D471 (2014).
55. Teumer, A. Common methods for performing Mendelian randomization. *Front. Cardiovasc. Med.* **5**, 51 (2018).
56. Permutt, T. & Hebel, J. R. Simultaneous-equation estimation in a clinical trial of the effect of smoking on birth weight. *Biometrics* **45**, 619–622 (1989).
57. Zhu, Z. et al. Causal associations between risk factors and common diseases inferred from GWAS summary data. *Nat. Commun.* **9**, 224 (2018).
58. Burgess, S., Butterworth, A. & Thompson, S. G. Mendelian randomization analysis with multiple genetic variants using summarized data. *Genet. Epidemiol.* **37**, 658–665 (2013).
59. Bowden, J. et al. A framework for the investigation of pleiotropy in two-sample summary data Mendelian randomization. *Stat. Med.* **36**, 1783–1802 (2017).
60. Bowden, J., Davey Smith, G. & Burgess, S. Mendelian randomization with invalid instruments: effect estimation and bias detection through Egger regression. *Int. J. Epidemiol.* **44**, 512–525 (2015).
61. Bowden, J. et al. Assessing the suitability of summary data for two-sample Mendelian randomization analyses using MR-Egger regression: the role of the I^2 statistic. *Int. J. Epidemiol.* **45**, 1961–1974 (2016).
62. Bowden, J., Davey Smith, G., Haycock, P. C. & Burgess, S. Consistent estimation in Mendelian randomization with some invalid instruments using a weighted median estimator. *Genet. Epidemiol.* **40**, 304–314 (2016).
63. Hartwig, F. P., Davey Smith, G. & Bowden, J. Robust inference in summary data Mendelian randomization via the zero modal pleiotropy assumption. *Int. J. Epidemiol.* **46**, 1985–1998 (2017).

Acknowledgements

We are sincerely grateful for the support provided by China National GeneBank. We thank all the volunteers for their time and for self-collecting the fecal samples using our kit. We are very grateful to K. Kristiansen (Department of Biology, University of Copenhagen, Denmark; BGI-Qingdao, BGI-Shenzhen, China) for his support for the joint PhD program.

Author contributions

H.J. and T.Z. conceived and organized this study. J.W. initiated the overall health project. X.X., H.Y., S.Z., Y.H., W.L. and Y. Zong contributed to organization of the cohort sample collection and questionnaire collection. H.L. led the DNA extraction and sequencing. X.Q., J.Z. and R.W. generated the metabolic data. X. Liu, T.Z. and X.T. processed the whole-genome data. Y. Zou, X. Lin, Z.Z., H.Z., L.T., Q.W., Z.J. and L.X. processed the metagenome data. X. Liu and X.T. performed the Mendelian randomization analyses. X. Liu and H.J. wrote the manuscript. All authors contributed to the data and text in this manuscript.

Competing interests

The authors declare no competing interests.

Additional information

Supplementary information The online version contains supplementary material available at https://doi.org/10.1038/s41588-021-00968-y.

Correspondence and requests for materials should be addressed to Huijue Jia or Tao Zhang.

Peer review information *Nature Genetics* thanks Yukinori Okada and the other, anonymous, reviewer(s) for their contribution to the peer review of this work.

nature research

Corresponding author(s): Tao Zhang && Huijue Jia

Last updated by author(s): Oct 1, 2021

Reporting Summary

Nature Research wishes to improve the reproducibility of the work that we publish. This form provides structure for consistency and transparency in reporting. For further information on Nature Research policies, see Authors & Referees and the Editorial Policy Checklist.

Statistics

For all statistical analyses, confirm that the following items are present in the figure legend, table legend, main text, or Methods section.

n/a	Confirmed	
☐	☒	The exact sample size (*n*) for each experimental group/condition, given as a discrete number and unit of measurement
☐	☒	A statement on whether measurements were taken from distinct samples or whether the same sample was measured repeatedly
☐	☒	The statistical test(s) used AND whether they are one- or two-sided *Only common tests should be described solely by name; describe more complex techniques in the Methods section.*
☐	☒	A description of all covariates tested
☐	☒	A description of any assumptions or corrections, such as tests of normality and adjustment for multiple comparisons
☐	☒	A full description of the statistical parameters including central tendency (e.g. means) or other basic estimates (e.g. regression coefficient) AND variation (e.g. standard deviation) or associated estimates of uncertainty (e.g. confidence intervals)
☐	☒	For null hypothesis testing, the test statistic (e.g. *F*, *t*, *r*) with confidence intervals, effect sizes, degrees of freedom and *P* value noted *Give P values as exact values whenever suitable.*
☒	☐	For Bayesian analysis, information on the choice of priors and Markov chain Monte Carlo settings
☐	☒	For hierarchical and complex designs, identification of the appropriate level for tests and full reporting of outcomes
☐	☒	Estimates of effect sizes (e.g. Cohen's *d*, Pearson's *r*), indicating how they were calculated

Our web collection on statistics for biologists contains articles on many of the points above.

Software and code

Policy information about availability of computer code

Data collection	No software was used for data collection.
Data analysis	The host genome reads were aligned to the latest reference human genome GRCh38/hg38 with BWA (v.0.7.15; http://bio-bwa.sourceforge.net/). The alignments were indexed in the BAM format using Samtools (v.0.1.18; http://samtools.sourceforge.net/) and PCR duplicates were marked for downstream filtering using Picardtools (v.1.62; http://broadinstitute.github.io/picard/). The genome variants calling were performed using GATK (v3.8; https://gatk.broadinstitute.org/hc/en-us). The low-depth data were imputed using BEAGLE (v.5.0; https://faculty.washington.edu/browning/beagle/b5_0.html). The metagenome reads were aligned to hg38 using SOAP (v.2.22; http://soap.genomics.org.cn). Quality control, association analyses and genetic risk score analyses were performed in PLINK (v1.90; http://zzz.bwh.harvard.edu/plink/). Variance explained analysis was performed using REML model in GCTA (v.1.26.0; https://cnsgenomics.com/software/gcta). One-sample MR analyses were performed using TSLS method in AER package (v1.2-9; https://www.rdocumentation.org/packages/AER/versions/1.2-9/topics/ivreg). Two-sample MR analyses were performed in GSMR (v1.0.7; http://cnsgenomics.com/software/gsmr/) and TwoSampleMR (v.0.5.6; https://mrcieu.github.io/TwoSampleMR/). All statistics analyses and visualizations were performed in R (v.3.2.5; https://www.r-project.org).

For manuscripts utilizing custom algorithms or software that are central to the research but not yet described in published literature, software must be made available to editors/reviewers. We strongly encourage code deposition in a community repository (e.g. GitHub). See the Nature Research guidelines for submitting code & software for further information.

Data

Policy information about availability of data

All manuscripts must include a data availability statement. This statement should provide the following information, where applicable:

- Accession codes, unique identifiers, or web links for publicly available datasets
- A list of figures that have associated raw data
- A description of any restrictions on data availability

The human reference hg38 datasets were publicly available from http://hgdownload.soe.ucsc.edu/goldenPath/hg38/bigZips/. All summary statistics that support the findings of this study including the associations between host genetics and microbiomes, host genetics and metabolites are publicly available from https://ftp.cngb.org/pub/CNSA/data2/CNP0000794/. The release of the data was approved by the Ministry of Science and Technology of China (Project ID: 2020BAT1137). Individual-level data including host genetics, metagenomics and metabolites have been uploaded to the GSA database (https://ngdc.cncb.ac.cn/bioproject/browse/PRJCA005334). Access to individual-level data has to be approved by corresponding authors (tao.zhang@genomics.cn, jiahuijue@genomics.cn), and is subject to the policies and approvals from the Human Genetic Resource Administration, Ministry of Science and Technology of the People's Republic of China. The summary statistics data for 42 diseases and 59 blood quantitative traits in 212,453 Japanese individuals were available from Biobank Japan (http://jenger.riken.jp/en/result).

Field-specific reporting

Please select the one below that is the best fit for your research. If you are not sure, read the appropriate sections before making your selection.

☒ Life sciences ☐ Behavioural & social sciences ☐ Ecological, evolutionary & environmental sciences

For a reference copy of the document with all sections, see nature.com/documents/nr-reporting-summary-flat.pdf

Life sciences study design

All studies must disclose on these points even when the disclosure is negative.

Sample size	No sample size calculation was performed prior this study. We used a total of 3,432 samples that were currently available from 4D-SZ cohort, and processed using statistical method and sample exclusion criteria which is clearly described in the text and in the Methods section. The identified suggestive genetic variants (p<1e-5) explained a median value of 24.9% variance for microbial features and a median of 28.6% variance for metabolic traits, suggesting an enough power of our samples for MR analyses in this study.
Data exclusions	For discovery cohort, samples were excluded if meet any of these criteria: (i) mean sequencing depth ≤ 20×; (ii) variant call rate ≤ 98%; (iii) existing population stratification by performing principal components analysis (PCA) analysis implemented in PLINK50 (version 1.07) and (iv) having related individuals by calculating pairwise identity by descent (IBD, Pi-hat threshold 0.1875) in PLINK. Only 10 samples were removed in quality control filtering. We applied several strict exclusion thresholds for variants: (i) mean depth ≤ 8×; (ii) Hardy-Weinberg equilibrium (HWE) P ≤ 10-5; and (iii) genotype calling rate ≤ 98%. For replication cohort, samples were removed if the mean sequencing depth ≤ 6×, variant call rate ≤ 98%, or existing population stratification or having kinship. We excluded variants with imputation info. ≤ 0.7, Hardy-Weinberg equilibrium P ≤ 10-5 or genotype calling rate ≤ 90%. The details were described in the methods.
Replication	We did a two-part replication. First, we replicated the significant genetic variants identified in discovery cohort using replication dataset. For example, among the 6,541 mQTLs identified in the discovery cohort, 5,088 variants were covered by the replication dataset. Especially for the 174 genome-wide and 39 study-wide significant associations, we could replicate 51 and 29 associations in the same direction (P < 0.05), respectively. Second, we replicated the significant MR signals identified in discovery cohort using replication dataset. We performed direct correlation analysis between metabolic traits and microbial features and found the observationally significant associations, and limited the causality analyses to these. Furthermore, we used an one-sample and six different two-sample MR methods to further confirm the observationally significant causal relationships. Finally, 43 of the 58 hits identified using one-sample MR in discovery cohort were replicated in the replication cohort.
Randomization	This is not an expertimental study. Randomization is not applicable
Blinding	This is not an experimental study. Blinding is not applicable

Reporting for specific materials, systems and methods

We require information from authors about some types of materials, experimental systems and methods used in many studies. Here, indicate whether each material, system or method listed is relevant to your study. If you are not sure if a list item applies to your research, read the appropriate section before selecting a response.

Materials & experimental systems

n/a	Involved in the study
☒	☐ Antibodies
☒	☐ Eukaryotic cell lines
☒	☐ Palaeontology
☒	☐ Animals and other organisms
☐	☒ Human research participants
☒	☐ Clinical data

Methods

n/a	Involved in the study
☒	☐ ChIP-seq
☒	☐ Flow cytometry
☒	☐ MRI-based neuroimaging

Human research participants

Policy information about studies involving human research participants

Population characteristics	The 4D-SZ cohort is an extensive dataset of self-reported metadata, as well as blood and stool samples, had been collected during physical examination. Mean age is 29 years (SD=6.09 years) and 51% of individuals are female. This cohort have a total of 3,432 individuals. In discovery cohort, 2,002 individuals had blood samples for whole genome sequencing, of which 1,539 had fecal samples for whole metagenome sequencing. In replication cohort, 1,430 individuals had blood samples for whole genome sequencing, 1,006 out of which had fecal samples for whole metagenome sequencing.
Recruitment	Individuals were recruited independently of this study, and was based on voluntary participation after an invitation letter. All 4D-SZ individuals were Asian adults, and their average age was only 29 years old.
Ethics oversight	The study was approved by the Institutional Review Boards (IRB) at BGI-Shenzhen, and all participants provided written informed consent at enrollment. All study procedures were performed in accordance with the World Medical Association Declaration of Helsinki ethical principles for medical research.

Note that full information on the approval of the study protocol must also be provided in the manuscript.